# NUMERICAL MODELING ON SOLID CONE NOZZLE
# WITHOUT A VANE SWIRLER

by

## Mst. Shahin Akter Pervin



## KHULNA UNIVERSITY OF ENGINEERING & TECHNOLOGY, KHULNA 920300 BANGLADESH

**December, 2006**

# NUMERICAL MODELING ON SOLID CONE NOZZLE
# WITHOUT A VANE SWIRLER

by

**Mst. Shahin Akter Pervin**

A thesis/project submitted in partial fulfillment of the requirements for the degree of
Master of Science in Engineering in Department of Mechanical Engineering

Khulna University of Engineering & Technology
Khulna 920300, Bangladesh

December, 2006

# DECLARATION

This is to certify that the thesis/project work entitled "Numerical Modeling on Solid Cone Nozzle without a Vane Swirler" has been carried out by Mst. Shahin Akter Pervin in the Department of Mechanical Engineering, Khulna University of Engineering & Technology, Khulna, Bangladesh. The above research work or any part of the work has not been submitted anywhere for the award of any degree or diploma.
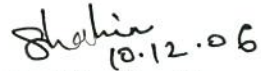
10.12.06

Signature of the Supervisor

Dr. Mihir Ranjan Halder

Professor

Department of Mechanical Engineering

Khulna University of Engineering & Technology

10.12.06

Signature of the Candidate

Name : Mst. Shahin Akter Pervin

Roll No : 0005502

# Approval

This is to certify that the thesis/project work submitted by Mst. Shahin Akter Pervin entitled "Numerical Modeling on Solid Cone Nozzle without a Vane Swirler" has been approved by the Board of Examiners for the partial fulfillment of the requirements for the degree of M. Sc. Engineering in the Department of Mechanical Engineering, Khulna University of Engineering & Technology, Khulna, Bangladesh in December, 2006.

## BOARD OF EXAMINERS

Dr. Mihir Ranjan Halder
Professor, Department of Mechanical Engineering
Khulna University of Engineering & Technology.

Chairman
(Supervisor)

08.03.07

Dr. Md. Syed Ali Molla
Professor & Head,
Department of Mechanical Engineering
Khulna University of Engineering & Technology

Member

8|3|

Dr. Md. Nawsher Ali Moral
Professor, Department of Mechanical Engineering
&
Vice-Chancellor
Khulna University of Engineering & Technology
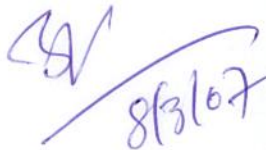
Member

Dr. Khandker Aftab Hossain
Professor, Department of Mechanical Engineering
Khulna University of Engineering & Technology

Member

08.3.07

Dr. A.K.M. Sadrul Islam
Professor
Department of Mechanical & Chemical Engineering
Islamic University of Technology, Board Bazar, Gazipur

Member
(External)

8|3|07

DEDICATED

TO

MY PARENTS

# ACKNOWLEDGEMENT

Date: 10.12.2006

Author

# ABSTRACT

The performance parameters like the coefficient of discharge $C_d$ and the spray cone angle $\psi$ of a swirl spray solid cone nozzle without a vane swirler have been studied numerically. The numerical computation of flow through the nozzle is performed by solving the conservation equations of mass and momentum using MAC (Marker and Cell) algorithm. The standard k-$\in$ model of turbulence is adopted for computations of turbulent quantities. The values of coefficient of discharge $C_d$ and spray cone angle $\psi$ have been evaluated from the radial distributions of velocity components of liquid flow at the nozzle exit. It has been observed that the coefficient of discharge $C_d$ remains almost independent and the spray cone angle $\psi$ decreases with the Reynolds number Re of the flow at inlet to the nozzle for a given flow ratio $q_r$ (the ratio of flow rate through inlet central port to the total flow through the nozzle), diameter ratios $D_2/D_1$ and $D_o/D_1$. It is also found to decrease $C_d$ and increase $\psi$ with the decrease in $D_T/D_1$ ratio for a given Re, $q_r$, , $D_2/D_1$ and $D_o/D_1$. Again, for a given Re, $D_2/D_1$ and $D_T/D_1$ an increase in flow ratio $q_r$ increases the value of $C_d$ and decreases the value of $\psi$. However, the influence of $q_r$ on $C_d$ is prominent at lower values of diameter ratios $D_2/D_1$ from 0.125 to 0.21 and the spray cone angle $\psi$ on the other hand, is almost uninfluenced of $q_r$ for all values of $D_2/D_1$ below 0.37, while $\psi$ increases when $D_2/D_1$ is increased beyond 0.37. The increase of $\psi$ is more prominent in the lower range of $q_r$. The solid cone nozzles without a vane swirler show similar trends of variation of performance parameters with the existing results of other authors on solid cone nozzle with a vane swirler. The nozzle without vane swirler produces lower values of $C_d$ and higher values of $\psi$ than those of nozzle with a vane swirler for the same conditions. The nozzle of the present work would be less costly and provides higher spray cone angle $\psi$ which could produce better atomization as well.

# CONTENTS

# LIST OF FIGUREAS

# NOMENCLATURE

| | |
|---|---|
| $A_o$ | Cross-sectional area of nozzle orifice (m$^2$) |
| $A_p$ | Total area of injection ports (m$^2$) |
| $C_d$ | Coefficient of Discharge |
| $C_\mu$ , $C_{1\varepsilon}$ , $C_{2\varepsilon}$ | Empirical constants of k-$\varepsilon$ equations |
| $D_1$ | Diameter of swirl chamber (m) |
| $D_2$ | Diameter of inlet central port (m) |
| $D_T$ | Diameter of tangential port (m) |
| $D_o$ | Diameter of orifice of the nozzle (m) |
| $k^/$ | Turbulent kinetic energy (Nm) |
| $k$ | Dimensionless $k^/$ ($k^/ / U^2$) |
| $p$ | Dimensionless $p^/$ ($p^/ / \rho U^2$) |
| $p^/$ | Pressure (N/m$^2$) |
| $p_a$ | Ambient Pressure (N/m$^2$) |
| $Q$ | Total flow rate (m$^3$/ sec) |
| $Q_2$ | Flow rate through central port (m$^3$/ sec) |
| $q_r$ | Flow ratio ($Q_2/Q$) |
| $r^/$ | Radial coordinate (m) |
| $r$ | Dimensionless $r^/$ ($r^/ / D_1$) |
| $R_1$ | Radius of swirl chamber (m) |
| $R_2$ | Radius of inlet central port (m) |
| $R_T$ | Radius of tangential port (m) |
| $R_o$ | Radius of the orifice (m) |
| $Re$ | Inlet Reynolds number ($\rho U D_1/\mu$) |

| | |
|---|---|
| U | Average Axial Velocity(m / sec) |
| $v'$ | Velocity (m / sec) |
| v | Dimensionless $v'$ ($v'$ / U ) |
| $z'$ | Axial coordinate (m) |
| z | Dimensionless $z'$ ($z'$ / $D_1$) |

**Greek Letters**

| | |
|---|---|
| $\alpha$ | Half cone angle of swirl chamber (degree) |
| $\psi$ | Spray cone angle (degree) |
| $\varepsilon'$ | Turbulent kinetic energy dissipation rate (Nm/sec) |
| $\varepsilon$ | Dimensionless $\varepsilon'$ ($\varepsilon'$ $D_1$/ $u_o^3$) |
| $\mu$ | Viscosity (N.sec/m$^2$) |
| $\rho$ | Density (kg/m$^3$) |

**Subscripts**

| | |
|---|---|
| r | In radial direction |
| z | In axial direction |
| $\theta$ | In azimuthal direction |

# CHAPTER 1

# INTRODUCTION

## 1.1 General Description and Practical Relevance

The swirl spray pressure nozzle is used in the field of combustion, drying, humidification, cooling, air-conditioning, sprinkling etc. The simplest form of a pressure swirl nozzle is known as simplex nozzle. The basic purpose of a simplex nozzle in its field of application is to produce a widely dispersed spray of atomized liquid having a very high value of specific surface area (surface area per unit volume). This enhances the rate of heat and mass transfer between the dispersed liquid phase and the ambient gas phase in the fields of application as mentioned above. A tangential component of velocity is imparted to the liquid at entry to such nozzles, and the liquid attaining a swirling motion inside the nozzle emanates in the form of a conical liquid sheet or jet in the surrounding ambience. The sheet or jet, due to its inherent hydrodynamic instability, disintegrates into ligaments and finally into liquid drops in the form of a well defined atomized spray. The performance characteristics of such nozzle are the coefficient of discharge and the spray cone angle. There are two basic types of simplex nozzle. In one type, liquid at high pressure is supplied to swirl chamber of the nozzle through purely tangential ports and the nozzle produces a hollow cone spray. In another type, a high pressure liquid enters to the swirl chamber partly through a central cylindrical port which provides a pure axial type entry and partly through an annular vane swirler which imparts swirl to the liquid at inlet. The nozzle, under the situation, produces a solid cone spray. A simple form of a solid cone spray nozzle is shown in Fig.1.1. A solid cone or full cone spray contains significant drop mass flux throughout the spray width. They are commonly produced by twin fluid atomization techniques. While the hollow cone spray nozzles are mostly used in power industries including aviation and space technology, the solid cone spray nozzles are largely employed in gas scrubbing, coke quenching, spray drying, sprinkling, chemical processing, rinsing and agricultural fields.

The design approach of such nozzles requires the interrelations between different performance characteristics of the nozzle with pertinent input parameters such as, liquid properties, injection conditions and nozzle geometry. This needs a physical understanding of the flow inside the nozzle and mechanism of spray formation outside the nozzle.
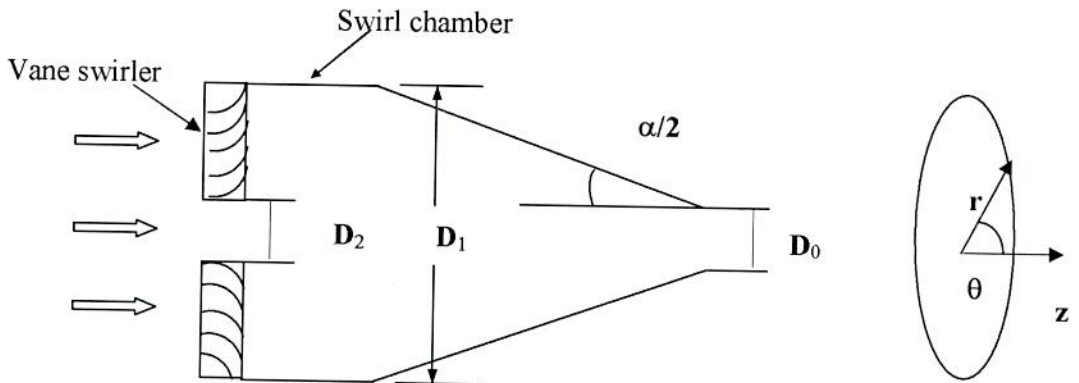


**Fig. 1.1 The geometry of a solid cone spray nozzle**

Generally in solid cone nozzle, fluid gets axial velocity from the flow through central axial port and tangential velocity from the flow through a vane swirler which in fact provides both tangential and axial components of velocity. The tangential component of velocity is responsible to increase the spray cone angle of the final spray. A solid cone nozzle could be made whose axial velocity comes from the axial flow through the central port and tangential velocity comes from the flow through the tangential entry ports placed symmetrically at the periphery of the swirl chamber as shown in Fig.1.2,. then the nozzle under such entries replaces the vane swirler for getting tangential velocity could simplify the manufacturing process as well as the cost of a solid cone nozzle.
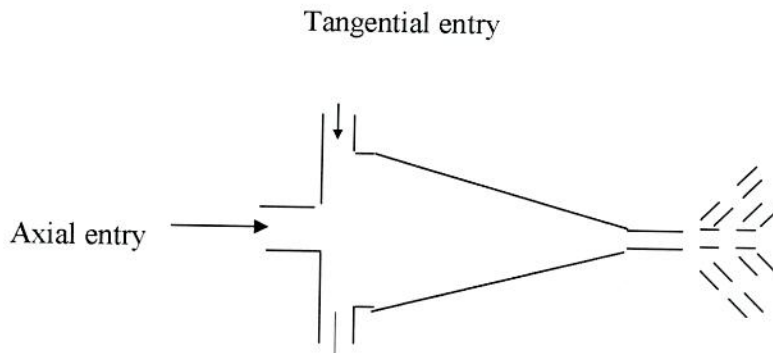


**Fig. 1. 2 The geometry of a Solid cone spray nozzle without a vane Swirler**

2

## 1.2 Objectives

The objectives of the project work are chosen as

1) Numerical modeling of a solid cone nozzle without a vane swirler.

2) Comparison of the results from numerical computations with the published results.

# CHAPTER 2

## LITERATURE REVIEW

### 2.1 Atomizing Nozzles

The transformation of bulk liquid into sprays and other physical dispersions of small particles in a gaseous atmosphere are of importance in several industrial processes and has many other applications in agriculture, meteorology and medicine. Numerous spray devices have been developed for the purpose and they are generally designated as atomizers or nozzles. The process of atomization is one in which a liquid jet or sheet is disintegrated by the kinetic energy of the liquid itself or by exposure to high velocity ambient air or gas or as a result of mechanical energy applied externally through a rotating or vibrating device. Because of the random nature of the atomization process the resultant spray is usually characterized by a wide spectrum of drop sizes.

Natural sprays include waterfall mists, rains and ocean sprays. In the home, sprays are produced by showerheads, garden hoses and hair sprays. They are commonly used in applying agricultural chemicals to crops, paint spraying, spray drying of wet solids, food processing, cooling of nuclear cores, gas-liquid mass transfer applications, dispersing liquid fuels for combustion and many other applications.

Combustion of liquid fuels in diesel engines, spark ignition engines, gas turbines, rocket engines and industrial furnaces is dependent on effective atomization to increase the specific surface area of the fuel and there by achieve high rates of mixing and evaporation. In most combustion systems, reduction in mean fuel drop size leads to higher volumetric heat release rates, easier light up, a wider burning range and lower exhaust concentrations of pollutant emissions. In other applications, however, such as crop spraying, small droplets must be avoided because their settling velocity is low and under certain meteorological conditions, they can drift too far downwind. Drop sizes are also important in spray drying and must be closely controlled to achieve the desired rates of heat and mass transfer.

4

## 2.2 Types of Nozzle

Sprays may be produced in various types of nozzles. According to Lefebvre [1989] the nozzles are mainly classified as

   (i) Pressure nozzles

   (ii) Rotary nozzles

   (iii) Air-Assist nozzles

   (iv) Air blast nozzles and

   (v) Other types

### 2.2.1 Pressure Nozzles

In a pressure nozzle, a liquid is discharged through a small aperture under high-applied pressure and the pressure energy is converted into kinetic energy (velocity) hence produces spray of liquid. For a typical hydrocarbon fuel, in the absence of frictional losses a nozzle pressure drop of 138 kPa(20 psi) produces an exit velocity of 18.6 m/s. As velocity increases as the square root of the pressure, at 689 kPa (100 psi) a velocity of 41.5 m/s is obtained, while 5.5 MPa (800 psi) produces 117 m/s.

Pressure nozzles are again classified as

a. Plain orifice nozzle

b. Pressure-swirl (simplex) nozzle

c. Square spray nozzle

d. Duplex nozzle

e. Dual orifice nozzle

f. Spill return nozzle

g. Fan spray nozzle

**a. Plane orifice nozzle:** A simple circular orifice is used to inject a round jet of liquid into the surrounding air. Finest atomization is achieved with small orifices. Combustion applications for plain orifice nozzles include turbojet afterburners, ramjets, diesel engines and rocket engines.

**b. Pressure-swirl (simplex) nozzle:** A circular outlet orifice is preceded by a swirl chamber into which liquid flows through either a number of tangential holes or both tangential and axial holes. The spray is produced under the situation with a wide angle giving a greater specific area. There are two basic types of pressure swirl nozzles, such as

Hollow cone spray nozzle and

Solid cone spray nozzle

Hollow cone spray nozzle: In a hollow cone spray nozzle, liquid at high pressure is supplied to the nozzle through tangential entry ports only and is finally discharged from an outlet orifice in the form of a hollow cone spray. The swirling flow of liquid creates a core of air or ambient gas that extends from the discharge orifice to the rear of the swirl chamber. The geometry of the nozzle is usually a converging passage followed by a short cylindrical orifice. Sometimes, the geometry of a hollow cone swirl nozzle is a narrow cylindrical one, which is employed as an injector of liquid oxygen of a co-axial liquid and gaseous propellant injector in a rocket engine.

Solid cone spray nozzle: In a solid cone nozzle, liquid at high pressure is fed to the nozzle having both axial and tangential velocities. Generally axial velocity comes from the flow through central axial entry port and tangential velocity originates from the flow through a vane swirler. This type of nozzle produces a solid or full cone spray comprising drops that are distributed fairly uniform throughout its volume. Solid cone sprays contain significant drop mass flux throughout the spray width. They are most commonly produced by twin fluid atomization techniques. However, in a certain cases it is inconvenient to use an atomizing gas and in some applications the drop mass flux and velocity achievable by twin fluid atomization are in adequate. Moreover, for many combustion applications, a solid cone nozzle is considered undesirable because it can give rise excessive concentration of soot and particulates in the exhaust gases. Examples of such nozzle applications include water spray cooling, in various processes associated with the manufacture of metal ingots and sheet, the descaling of surfaces and gas scrubbing, coke quenching, rinsing and agricultural fields etc.

**c. Square spray nozzle:** This is essentially a solid-cone nozzle, but the outlet orifice is specially shaped to distort the conical spray into a pattern that is roughly in the form of a square. Atomization quality is not as high as with conventional hollow cone nozzles but when used in multiple- nozzle combinations, a fairly uniform coverage of large areas can be achieved.

**d. Duplex nozzle:** A drawback of all types of pressure nozzles is that the liquid flow rate is proportional to the square root of the injection pressure differential. In practice, this limits the flow range of simplex nozzles to about 10:1. The duplex nozzle overcomes this limitation by feeding the swirl chamber through two sets of distributor slots, each having its own separate liquid supply. Duplex nozzles allow good atomization to be achieved over a range of liquid flow rates of about 40:1 without the need to resort to excessively high delivery pressures.

**e. Dual orifice nozzle:** This is similar to the duplex nozzle except those two separate swirl chambers are provided. One for the primary flow and the other for the secondary flow. The two swirl chambers are housed concentrically within a single nozzle body to form a "nozzle within a nozzle". Dual- orifice nozzles offer more flexibility than duplex nozzles.

**f. Spill return nozzle:** This is essentially a simplex nozzle, but with a return flow line at the rear or side of the swirl chamber and a valve to control the quantity of liquid removed from the swirl chamber and returned to supply line. Very high turndown ratios are attainable with this design. Atomization quality is always good because the supply pressure is held constant at a high value, reductions in flow rate being accommodated by adjusting the valve in the spill return line.

**g. Fan Spray nozzle:** Several different concepts are used to produce flat or fan-shaped sprays. The most popular type of nozzle is one in which the orifice is formed by the intersection of a V-groove with a hemispheric cavity communicating with a cylindrical liquid inlet. It produces a liquid sheet parallel to the major axis if the orifice, which disintegrates into a narrow elliptical spray.

### 2.2.2 Rotary Atomizer

One widely used type of rotary nozzle comprises a high- speed rotating disk with means for introducing liquid at its center. The liquid flows radially outward across the disk and is discharged at high velocity from its periphery. The disk may be smooth and flat or may have vanes or slots to guide the liquid to the periphery. At low flow rates, droplets form near the edge of the disk. At high flow rates, ligaments or sheets are generated at the edge and disintegrate into droplets. In contrast to pressure nozzles, rotary atomizers allow independent variation of flow rate and disk speed, thereby providing more flexibility in operation.

### 2.2.3 Air-Assist Nozzle

In this type of nozzle the liquid is exposed to a stream of air or steam flowing at high velocity. In the internal mixing configuration, gas and liquid mix within the nozzle before discharging through the outlet orifice. The liquid is sometimes supplied through tangential slots to encourage a conical discharge pattern. However, the maximum spray angle is limited to about $60^0$. The device tends to be energy inefficient, but it can produce a finer spray than simple pressure nozzles.

### 2.2.4 Airblast Nozzle

These device's function is very similar manner to air assist nozzles, and both types fall in the general category of twin fluid atomizers. The main difference between air assist and airblast nozzles is that the former use relatively small quantities of air or steam flowing at very high velocities (usually sonic), whereas the latter employ large amounts of air flowing at much lower velocities (<100m/s). Airblasts nozzles are thus ideally suited for atomizing liquid fuels in continuous-flow combustion systems, such as gas turbines, where air velocities of this magnitude are usually readily available.

## 2.2.5 Other Types

Most practical nozzles are of the pressure, rotary or twin-fluid type. However, many other forms of nozzles have been developed that are useful in special applications. These are as follows: -

Electrostatic

Ultrasonic

Sonic(whistle)

Windmill

Vibrating capillary

Flashing liquid jets

Effervescent atomization

## 2.3 CFD (Computational Fluid Dynamics)

Computers might make the study of fluid flow easier and more effective. Once the power of computers had recognized, interest in numerical techniques was increased dramatically. Solution of the equations of fluid mechanics on computers has become so important that it now occupies the attention of perhaps a third of all researchers in fluid mechanics and the proportion is still increasing. This field is known as Computational Fluid Dynamics (CFD). To obtain an approximate solution numerically, one has to use a discretization method which approximates the deferential equations by a system of linear algebraic equations, which can then be solved on a computer. The approximations are applied to small domains in space and/or time so the numerical solution provides results at discrete locations in space and time. Much as the accuracy of experimental data depends on the quality of the tools used, the accuracy of numerical solutions is dependent on the quality of discretizations used. There are many approaches, but the most important of which are :

Finite difference (FD) Method

Finite volume ( FV) Method

Finite element (FE) Method

### 2.3.1 Finite Difference Method (FD)

This is the oldest method for numerical solution of partial differential equations, believed to have been introduced by Euler in the 18th century. It is also the easiest method to use for simple geometries. The starting point is the conversion of differential equation in approximate finite difference form. The solution domain is subdivided into a number grid. In principle, the FD method can be applied to any grid type. However, in most of the applications of the FD method, it has been applied to the structured grids. On the structured grids, the FD method is very simple and effective. It is especially easy to obtain higher-order schemes on regular grids. Applying approximate finite difference form of equation at each grid point, one algebraic equation for each grid node is obtained in which the variables at that node and a certain number of neighbor nodes appear as unknowns.

Then boundary conditions are applied for all boundary nodes. After setting initial values for all the unknown grid nodes a solution method for linear algebraic equations is applied to obtain the solution of all unknowns.

### 2.3.2 Discretization

**Elementary Finite Difference Quotients**

Finite difference representations of derivatives are derived from Taylor series expansions. For example, if $u_{i,j}$ is the x-component of velocity at point (i, j) in a 2D system as shown in Fig. 2.1, then the velocity $u_{i+1,j}$ at point (i+1,j) can be expressed in terms of Taylor series expansion about point (i,j) as

$$u_{i+1,j} = u_{i,j} + \left(\frac{\partial u}{\partial x}\right)_{i,j} \Delta x + \left(\frac{\partial^2 u}{\partial x^2}\right)_{i,j} \frac{(\Delta x)^2}{2!} + \left(\frac{\partial^3 u}{\partial x^3}\right)_{i,j} \frac{(\Delta x)^3}{3!} + \dotsb \qquad 2.1$$

Mathematically Eqn. 2.1 is an exact expression for $u_{i+1,j}$ if the series converges. In practice, $\Delta x$ is small and any higher order term of $\Delta x$ is smaller than $\Delta x$. Hence for any function u(x), Eqn 2.1 can be truncated after a finite number of terms. For example, if terms of magnitude $(\Delta x)^3$ and higher order are neglected, Eqn. 2.1 becomes

$$u_{i+1,j} \approx u_{i,j} + \left(\frac{\partial u}{\partial x}\right)_{i,j} \Delta x + \left(\frac{\partial^2 u}{\partial x^2}\right)_{i,j} \frac{(\Delta x)^2}{2!} + \dots\dots \quad\quad 2.2$$



**Fig. 2.1 Discrete grid points around P(i,j)**

Eqn. 2.2 is second-order accurate, because terms of order $(\Delta x)^3$ and higher order have been neglected. If terms of order $(\Delta x)^2$ and higher order are neglected, Eqn. 2.1 is reduced to

$$u_{i+1,j} \approx u_{i,j} + \left(\frac{\partial u}{\partial x}\right)_{i,j} \Delta x \quad\quad 2.3$$

Eqn. 2.3 is first order accurate. In Eqns 2.2 and 2.3 the neglected higher-order terms represent the truncation error. Therefore, the truncation errors for Eqns. 2.2 and 2.3 are

$$\sum_{n=3}^{\infty}\left(\frac{\partial^n n}{\partial x^n}\right)_{i,j} \frac{(\Delta x)^n}{n!}$$

and

11

$$\sum_{n=2}^{\infty} \left( \frac{\partial^n n}{\partial x^n} \right)_{i,j} \frac{(\Delta x)^n}{n!}$$

It is now obvious that the truncation error can be reduced by retaining more terms in the Taylor series expansion of the corresponding derivative and reducing the magnitude of $\Delta x$.

From Eqn. 2.1,

$$\left( \frac{\partial u}{\partial x} \right)_{i,j} = \frac{u_{i+1,j} - u_{i,j}}{\Delta x} - \left( \frac{\partial^2 u}{\partial x^2} \right)_{i,j} \frac{\Delta x}{2} - \left( \frac{\partial^3 u}{\partial x^3} \right)_{i,j} \frac{(\Delta x^2)}{6} + \dots$$

or

$$\left( \frac{\partial u}{\partial x} \right)_{i,j} = \frac{u_{i+1,j} - u_{i,j}}{\Delta x} + O(\Delta x) \qquad\qquad 2.4$$

In Eqn. 2.4, the symbol $O(\Delta x)$ is a formal mathematical nomenclature that means "terms of order of $\Delta x$". In Eqn. 2.4 the order of magnitude of the truncation error is denoted by O. The first-order-accurate difference representation for the derivative $(\partial u / \partial x)_{i,j}$ expressed by Eqn. 2.4 can be identified as a first- order forward difference formula.

Again Taylor series expansion for $u_{i-1,j}$, about $u_{i,j}$:

$$u_{i-1,j} = u_{i,j} + \left( \frac{\partial u}{\partial x} \right)_{i,j} (-\Delta x) + \left( \frac{\partial^2 u}{\partial x^2} \right)_{i,j} \frac{(-\Delta x)^2}{2!} + \left( \frac{\partial^3 u}{\partial x^3} \right)_{i,j} \frac{(-\Delta x)^3}{3!} + \dots$$

or

$$u_{i-1,j} = u_{i,j} - \left( \frac{\partial u}{\partial x} \right)_{i,j} \Delta x + \left( \frac{\partial^2 u}{\partial x^2} \right)_{i,j} \frac{(\Delta x)^2}{2!} - \left( \frac{\partial^3 u}{\partial x^3} \right)_{i,j} \frac{(\Delta x)^3}{3!} + \dots \qquad 2.5$$

solving for $(\partial u / \partial x)_{i,j}$, we obtain

$$\left( \frac{\partial u}{\partial x} \right)_{i,j} = \frac{u_{i,j} - u_{i-1,j}}{\Delta x} + O(\Delta x) \qquad\qquad 2.6$$

Eqn. 2.6 is a first-order backward or rearward difference formula for the derivative $(\partial u / \partial x)$ at grid point (i,j).

Now subtracting Eqn. 2.5 from Eqn. 2.1

$$u_{i+1,j} - u_{i-1,j} = 2\left(\frac{\partial u}{\partial x}\right)_{i,j} \Delta x + \left(\frac{\partial^3 u}{\partial x^3}\right)_{i,j} \frac{(\Delta x)^3}{3} + \ldots\ldots\ldots \qquad 2.7$$
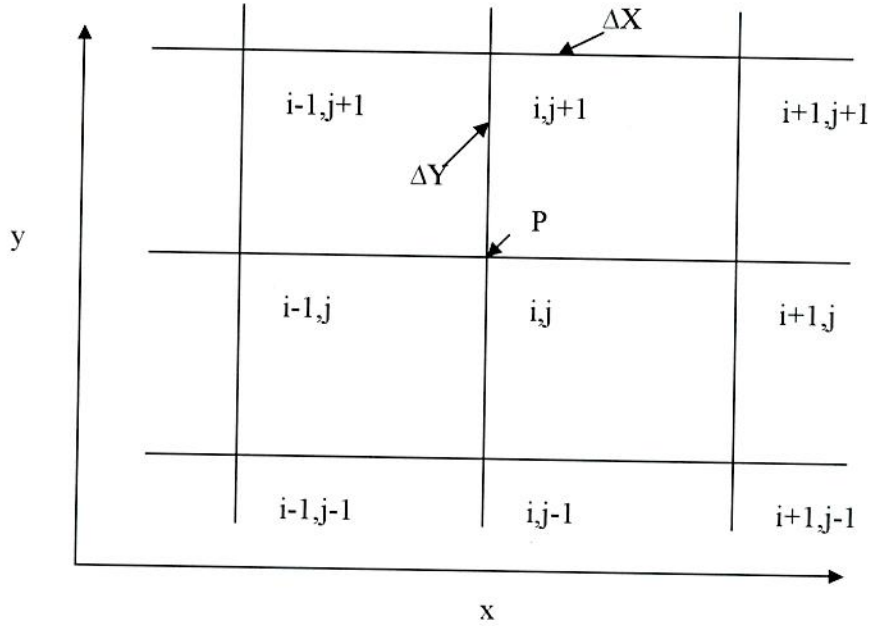
and solving for $(\partial u / \partial x)_{i,j}$ from Eqns. 2.7,

$$\left(\frac{\partial u}{\partial x}\right)_{i,j} = \frac{u_{i+1,j} - u_{i-1,j}}{2\Delta x} + O(\Delta x)^2 \qquad 2.8$$

Eqn. 2.8 is a first-order central difference formula for the derivative $(\partial u / \partial x)$ at grid point (i,j).

For a finite difference expression of the second-order partial derivative $(\partial^2 u / \partial x^2)_{i,j}$, Eqns. 2.1 and 2.5 are added which produces

$$u_{i+1,j} + u_{i-1,j} = 2u_{i,j} + \left(\frac{\partial^2 u}{\partial x^2}\right)_{i,j} (\Delta x)^2 + \left(\frac{\partial^4 u}{\partial x^4}\right)_{i,j} \frac{(\Delta x)^4}{12} + \ldots\ldots \qquad 2.9$$

or,

$$\left(\frac{\partial^2 u}{\partial x^2}\right)_{i,j} = \frac{u_{i+1,j} - 2u_{i,j} + u_{i-1,j}}{(\Delta x)^2} + O(\Delta x)^2 \qquad 2.10$$

Eqn. 2.10 is a second-order central difference formula for the derivative $(\partial^2 u / \partial x^2)$ at grid point (i,j).

Difference quotients for the y-derivatives are obtained in exactly the similar way. The results are analogous to the expressions for the x-derivatives as

$$\left(\frac{\partial u}{\partial y}\right)_{i,j} = \frac{u_{i,j+1} - u_{i,j}}{\Delta y} + O(\Delta y) \qquad \text{(Forward difference)}$$

$$\left(\frac{\partial u}{\partial y}\right)_{i,j} = \frac{u_{i,j} - u_{i,j-1}}{\Delta y} + O(\Delta y) \qquad \text{(Backward difference)}$$

$$\left(\frac{\partial u}{\partial y}\right)_{i,j} = \frac{u_{i,j+1} - u_{i,j-1}}{2\Delta y} + O(\Delta y)^2 \qquad \text{(Central difference)}$$

$$\left(\frac{\partial^2 u}{\partial y^2}\right)_{i,j} = \frac{u_{i,j+1} - 2u_{i,j} + u_{i,j-1}}{(\Delta y)^2} + O(\Delta y)^2 \qquad \text{(Central difference)}$$

13

## 2.4 MAC (Marker and Cell) Algorithm

The MAC method of Harlow and Welch [1965] is one of the earliest and most useful method for solving full Navier-Stokes equations. This method necessarily deals with a Poisson's equation for the pressure and Momentum equations for the computation of velocity. It was basically developed to solve the problems with free surfaces, but can be applied to any incompressible fluid flow problem. A modified version of the original MAC method due of Hirt and Cook [1972] has been used by many researchers to solve a variety of fluid flow problems. In this method, staggered grid system (where the scallers are defined at cell centre and vectors are defined at cell faces) is used and for pressure correction, continuity equation is satisfied by an iterative method instead of solving Poission's equation, following Hirt and Cook [1972] and Hirt et al. [1975]. The important ideas on which the MAC algorithm is based are:

1. Unsteady Navier-Stokes equations for incompressible flow in weak conservative from and the continuity equation are the governing equations.

2. Description of the problem is elliptic in space and parabolic in time. Solution will be marched in the time direction. At each time step, a converged solution in space domain is obtained but this converged solution at any time step may not be the solution of the physical problem.

3. If the problem is steady, in its physical sense, then after a finite number of steps in time direction, two consecutive time-steps will show identical solutions. However, in a machine-computation this is not possible hence a very small value say "STAT" is predefined. Typically, STAT may be chosen between $10^{-3}$ and $10^{-5}$. If the maximum discrepancy of any of the velocity components for two consecutive time steps at any location over the entire space does not exceed "STAT" then it can be said that the steady solution has been evolved.

4. If the physical problem is basically unsteady in nature, the aforesaid maximum discrepancy of any dependent variable for two consecutive time steps will never be less than "STAT". However, for a such situation, a velocity component can be stored over a long duration of time and plot of the velocity component against time depicts the character of flow. Such a flow may be labeled as simply "unsteady".

5. With the help of momentum equation, a provisional value of the velocity components is explicitly computed for the next time step.

6. Boundary conditions are to be applied after each explicit evaluation for the time step is accomplished. Since the governing equations are elliptic in space, boundary conditions on all confining surfaces are required. Moreover, the boundary conditions are also to be applied after every pressure-velocity iteration. The five principal kinds of boundary conditions to be considered are rigid no-slip walls, free-slip walls, in flow and outflow boundaries, and periodic boundaries.

## 2.5 Previous Works on Atomizing Nozzles

A review of literature of previous works pertaining to the field of swirl nozzle has been made in this section. Instead of a general and routine description of all the earlier works, a critical review of the relevant literature up to the date is presented.

A host of articles in the area of swirl nozzle is available in literature today. Most of the works pertain to the studies on hollow cone spray nozzle and are empirical and semi-empirical in nature. The pioneering work in the field was due to Taylor [1948] who gave the most valid theory for the potential flow through a swirl nozzle and predicted that the air core diameter and the spray cone angle were the inverse functions, while the coefficient of discharge was a direct function of a single dimensionless quantity defined as nozzle constant ($K = A_p / D_o D_1$), where $A_p$ was the area of tangential entry ports and $D_1$ and $D_o$ were the diameters of the swirl chamber and discharge orifice respectively. However, in a subsequent work, Taylor [1950], provided a theoretical treatment for the growth of boundary layer for a laminar swirling flow in a convergent duct.

The classical studies in the field of pressure swirl nozzle include those of Binnie and Harris [1950], Giffen and Massey [1950], Binnie and Harris [1950], Binne [1951], Cooke [1952], Tate and Marshall [1953], Talbot [1954], Radcliffe [1954], Binnie and Teare [1956], Binnie et al. [1957], and Nissan and Breson [1961]. Those works mostly referred to experimental investigations in the flow of swirling liquid through straight and convergent ducts. The investigations mostly included the experimental

determination of the distribution of pressure and different velocity components in the flow. In some of the above mentioned works, theoretical prediction of liquid film thickness was made either from the solution of potential flow or from the solution of boundary layer equations by momentum integral method. A good agreement of theoretical predictions of hydrodynamic parameters of nozzle flow and nozzle performance parameters with the experimental observations was hardly obtained in those works. Amongst the classical analytical works in the field of swirling flow, mention can be made of the work of Talbot [1954] who predicted the decay of a rotationally symmetric steady swirl superimposed on Poiseuille flow in a round pipe.

The developments in the field of simplex nozzle are mainly due to Kutty et al. [1978], Som and Mukherjee [1980a,b], Jones[ 1982], Som [1983a,b], Rizk and Lefebvre [1985a,b], Suyari and Lefebvre [1986],Wang and Lefebvre [1987], Chen et al. [1992], Keh-Chin et al. [1993], Yule at al. [1997], Holtzclaw et al. [1997], Jeng et al. [1998], Liao et al. [1999], Sakman et al. [2000], Datta and Som [2000], Dash et al. [2001], Halder et al. [2002, 2003], and Steinthorsson et al. [2000]. All these works brought about an understanding of the swirling flow inside a hollow cone spray nozzle and attempted to evaluate the liquid film thickness or air core diameter at the discharge orifice, the flow number, the coefficient of discharge and the spray cone angle of the nozzle from empirical studies, the simplified theoretical studies and numerical computations.

Kutty et al. [1978], experimentally studied on the flow number, the spray cone angle and the liquid film thickness at the discharge orifice of a hollow cone swirl nozzle. They determined the air core diameter from the measurement of liquid film thickness at the orifice and predicted that the air core diameter increased with an increase in the pressure drop till it became asymptotically maximum.

The works of Som and Mukherjee [1980a,b] and Som [1983a,b] referred to both theoretical and experimental investigations of air core diameter, the coefficient of discharge and the spray cone angle from a hollow cone swirl nozzle using Newtonian and power law non-Newtonian fluids. The nozzles considered for their studies did not

16

have a finite length of orifice. The theoretical analysis of their works was based on the solution of laminar boundary layer equations by momentum integral method. The theoretical predications did not agree well with the experimental observations.

The work of Rizk and Lefebvre [1985a] referred to a theoretical prediction of liquid film thickness at the discharge orifice of a conical swirl nozzle. The theory proposed by them was based on the force balance of a fluid element in a laminar flow along with the consideration of constant pressure gradient across the liquid film. The predictions of Rizk and Lefebvre [1985a] were found to be in good agreement with the experimental results of Kutty et al. [1978].

Suyari and Lefebvre [1986] measured the liquid film thickness at nozzle exit in their experimental investigation and compared their results with the available correlations. They observed that liquid film thickness increased with an increase in nozzle constant, K (as defined before ). Their experimental data were in good agreement with the predictions based on the analysis of Giffen and Muraszew [1953].

The main difficulty in the numerical simulation of flow in a hollow cone swirl nozzle is the accurate tracking of the interface between the two phases. Several methods for the solution of a free surface flow by interface tracking or interface capturing are available in the literature. Some of them are unable to give exact location of the interface and some of them are computationally expensive. Jeng et al. [1998], Liao et al. [1999] and Sakman et al. [2000] used a computational model based on Arbitrary Lagrangian – Eulerian (ALE) method for the simulation of flow in a hollow cone swirl nozzle. Jeng et al. [1998] simplified the simulation by treating the interface as an inviscid free surface. They observed a bulging shape of an air core at the entrance to orifice in a hollow cone swirl nozzle but did not report any quantitative or even qualitative functional relationship of the shape and size of the air core nozzle flow and nozzle geometry. Liao et al. [1999] and Sakman et al. [2000] investigated numerically the nozzle performance parameters like, the coefficient of discharge, the spray cone angle, and the liquid film thickness at nozzle outlet with geometrical parameters of the nozzle. They also compared their results with the corresponding experimental results of Jeng et

al. [1998]. and Sakman et al. [2000] and observed that the liquid film thickness at nozzle outlet decreased with an increase in the value of the ratio, $L_o/D_o$ where , $L_o$ was the length of orifice and $D_o$ was the diameter of orifice of the nozzle. However, this was in contrast to that obtained by Rizk and Lefebvre [1985a].

The recent work of Datta and Som [2000] predicted a uniform air core diameter in a hollow cone type conical swirl nozzle from a numerical solution of two-phase turbulent swirling flow in the nozzle. But in practice, the central air core is not uniform in size throughout the nozzle. Though the air core is of uniform cylindrical shape in the converging part of the nozzle, it bulges out at the entrance to the orifice and then again remains almost uniform within the short cylindrical orifice. The theory of Datta and Som [2000]  could not predict the bulging shape of an air core at the orifice. This may be attributed to the fact that the theory proposed by them, instead of providing a solution of a free surface flow, employed a minimum resistance principle in predicting the air core diameter from an optimization of nozzle flow with pressure drop for different arbitrary air core diameters superimposed in the flow.

Then Halder et al. [2003] predicted both numerically and experimentally, the shape and size of air core and its changes with geometry and flow condition from their detailed study on hollow cone swirl nozzle. They again reported the buldging shape of air core like Jeng et al. [1998] and determined its sizes as well. Halder et al. [2002] also reported about the initiation of air core within a hollow cone swirl nozzle.

From the above comprehensive review of literature, some information about the inception of air core in a hollow cone swirl nozzle and the influences of nozzle geometry and nozzle flow on the shape and size of a fully developed air core are obtained.

Even if a few information about air core in a conical nozzle are available in the literature as described above, but not much information in case of solid cone nozzle is found till date. The recent development in the field of solid cone nozzle with a vane swirler is mainly due to Nasr et al. [1999], Walmsley et al. [2000], and Halder et al.

[2004]. Nasr et al. [1999] found experimentally and gave empirical relations of droplet size, mean velocity and mass flux for the spray from the nozzle. Walmsley et al. [2000] from their numerical investigation, found the droplet and mass flux distribution in the spray from the solid cone nozzle. They described the modification, use and validation of a three-dimensional CFD code applied to model solid cone sprays produced by pressure swirl nozzles. The finite volume code used is a three dimensional, orthogonal, two-phase, Lagrangian tracking, transient code. It contains sub-models for the secondary break-up of droplets and for coalescence. The effect of chosen initial drop size distribution on the predicted fully developed spray characteristics is investigated. Optimum initial conditions are determined by making comparisons with published experimental data. Each initial distribution can be characterized by the maximum, minimum and Rosin-Rammler mean diameters. Relations are developed for these diameters as a function of the operating parameters.

Halder et al. [2004], investigated both numerically and experimentally on the coefficient of discharge $C_d$ and the spray cone angle $\Psi$ of a swirl spray solid cone pressure nozzle with a vane swirler. The theoretical predictions were made from a numerical computation of flow in the nozzle using the standard k-ε model of turbulence. The values of $C_d$ and $\Psi$ were evaluated from the radial distributions of velocity components of liquid flow at the nozzle exit. The experiments were carried out to measure the values of $C_d$ and $\Psi$ of a solid cone spray nozzle at different operating conditions to validate the numerical predictions. They established, from a fair agreement of values of $C_d$ and $\psi$ between their numerical and experimental results, that the adoption of the standard k-ε model for turbulence in nozzle flow serves well the purpose of predictions of $C_d$ and $\Psi$ within the range of operating parameters studied in their work.

In the present work, an attempt towards the numerical investigation on the co-efficient of discharge $C_d$ and the spray cone angle $\psi$ from a solid cone spray nozzle without a vane swirler as shown in Fig.1.2. has been made to carry out.

19

# CHAPTER 3

## THEORETICAL FORMULATION

The theoretical analysis refers to a typical solid cone spray swirl nozzle without a vane swirler is shown Fig.1.2. The entry of liquid to the nozzle is spilt through an axial central cylindrical port and two tangential ports at the base of swirl chamber. The standard k-∈ model with wall function treatment of turbulent quantities has been adopted for the computation of turbulent flow in the nozzle. This is done despite the fact, that many researchers have observed some shortcoming in the ability of the standard k-∈ model in predicting the recirculating and swirling flow results, at least quantitatively. The implementation of modified k-∈ models or higher order turbulence models (ASM,RSM) have been suggested by different researchers(Launder et al. [1977], Rodi [1979], Srinivasan and Mongia [1980], Fu et al. [1988], Jones and Pascau [1989] , Sturgess and Syed [1990], Nikjooy and Mongia [1991], Chang and Chen[ 1993]) in the computations of recirculating flows with improved accuracy. However, there is no conclusive information available in the literature regarding the accurate adoptability for any of such models in a confined swirling flow. The higher order turbulence models are relatively complex and time consuming and are found sometimes to be not accurate enough in predicting the strong swirling flows. Ramos [1985] in his numerical study on swirling stabilized combustor used the standard k-∈ model and argued that the consideration of a scalar viscosity in confined incompressible swirling flows was indeed adequate. Halder et al. [2004] reported that the reasonable accuracy in numerically predicted performance parameters like the coefficient of discharge and the spray cone angle in such swirling flow using standard k-∈ model was obtained comparing with their experimental values.

### 3.1 Governing Equations

The averaged conservation equations for the axi-symmetric flow of a liquid through the nozzle are written in a cylindrical coordinate system (Fig. 1.2) as

20

**Continuity Equation**

$$\frac{\partial v'_r}{\partial r'} + \frac{v'_r}{r'} + \frac{\partial v'_z}{\partial z'} = 0 \tag{3.1}$$

**Momentum Equations** :

r- Momentum

$$\frac{\partial v'_r}{\partial t'} + \frac{\partial}{\partial r'}\left(v_r'^2\right) + \frac{\partial}{\partial z'}\left(v'_r\, v'_z\right) + \frac{v_r'^2 - v_\theta'^2}{r'} =$$

$$-\frac{1}{\rho}\frac{\partial p'_1}{\partial r'} + \frac{2}{\rho}\frac{\partial}{\partial r'}\left(\mu'_{eff}\frac{\partial v'_r}{\partial r'}\right) + \frac{2}{r'}\frac{\mu'_{eff}}{\rho}\left(\frac{\partial v'_r}{\partial r'} - \frac{v'_r}{r'}\right)$$

$$+\frac{1}{\rho}\frac{\partial}{\partial z'}\left\{\mu'_{eff}\left(\frac{\partial v'_z}{\partial r'} + \frac{\partial v'_r}{\partial z'}\right)\right\} \tag{3.2}$$

z- Momentum

$$\frac{\partial v'_z}{\partial t'} + \frac{\partial}{\partial r'}\left(v'_r\, v'_z\right) + \frac{\partial}{\partial z'}\left(v_z'^2\right) + \frac{v'_r\, v'_z}{r'} =$$

$$-\frac{1}{\rho}\frac{\partial p'_1}{\partial z'} + \frac{1}{\rho}\frac{1}{r'}\frac{\partial}{\partial r'}\left\{r'\,\mu'_{eff}\left(\frac{\partial v'_z}{\partial r'} + \frac{\partial v'_r}{\partial z'}\right)\right\} + \frac{2}{\rho}\frac{\partial}{\partial z'}\left(\mu'_{eff}\frac{\partial v'_z}{\partial z'}\right) \tag{3.3}$$

θ- Momentum

$$\frac{\partial v'_\theta}{\partial t'} + \frac{\partial}{\partial r'}\left(v'_r\, v'_\theta\right) + \frac{\partial}{\partial z'}\left(v'_z\, v'_\theta\right) + \frac{2\, v'_r\, v'_\theta}{r'} =$$

$$\frac{1}{\rho}\frac{1}{r'^2}\frac{\partial}{\partial r'}\left\{r'^2\,\mu'_{eff}\left(\frac{\partial v'_\theta}{\partial r'} - \frac{v'_\theta}{r'}\right)\right\} + \frac{1}{\rho}\frac{\partial}{\partial z'}\left(\mu'_{eff}\frac{\partial v'_\theta}{\partial z'}\right) \tag{3.4}$$

where,

$$p'_1 = p' + 2/3\left(\rho k'\right)$$

$$\mu'_{eff} = \mu + \mu'_t$$

$$\mu'_t = c_\mu\,\rho k'^2 / \varepsilon'$$

**Turbulent Kinetic Energy Equation :**

$$\frac{\partial k'}{\partial t'} + \frac{\partial}{\partial r'}\left(v_r'\, k'\right) + \frac{\partial}{\partial z'}\left(v_z'\, k'\right) + \frac{v_r'\, k'}{r'} = \frac{1}{\rho}\frac{1}{r'}\frac{\partial}{\partial r'}\left(r'\frac{\mu_t'}{\sigma_k}\frac{\partial k'}{\partial r'}\right) + \frac{1}{\rho}\frac{\partial}{\partial z'}\left(\frac{\mu_t'}{\sigma_k}\frac{\partial k'}{\partial z'}\right) +$$

$$\frac{1}{\rho}\mu_t'\left[\begin{array}{l} 2\left\{\left(\dfrac{\partial v_r'}{\partial r'}\right)^2 + \left(\dfrac{v_r'}{r'}\right)^2 + \left(\dfrac{\partial v_z'}{\partial z'}\right)^2\right\} + \left(\dfrac{\partial v_\theta'}{\partial r'} - \dfrac{v_\theta'}{r'}\right)^2 \\ + \left(\dfrac{\partial v_r'}{\partial z'} + \dfrac{\partial v_z'}{\partial r'}\right)^2 + \left(\dfrac{\partial v_\theta'}{\partial z'}\right) \end{array}\right] - \varepsilon' \qquad\qquad 3.5$$

**Turbulent Kinetic Energy Dissipation Rate Equation :**

$$\frac{\partial \varepsilon'}{\partial t'} + \frac{\partial}{\partial r'}\left(v_r'\, \varepsilon'\right) + \frac{\partial}{\partial z'}\left(v_z'\, \varepsilon'\right) + \frac{v_r'\varepsilon'}{r'} = \frac{1}{\rho}\frac{\partial}{\partial r'}\left(r'\frac{\mu_t'}{\sigma_\varepsilon}\frac{\partial \varepsilon'}{\partial r'}\right) + \frac{1}{\rho}\frac{\partial}{\partial z'}\left(\frac{\mu_t'}{\sigma_\varepsilon}\frac{\partial \varepsilon'}{\partial z'}\right)$$

$$+ \frac{1}{\rho}c_{1\varepsilon}\frac{\varepsilon'}{k'}\mu_t'\left[2\left\{\left(\frac{\partial v_r'}{\partial r'}\right)^2 + \left(\frac{v_r'}{r'}\right)^2 + \left(\frac{\partial v_z'}{\partial z'}\right)^2\right\} + \left(\frac{\partial v_\theta'}{\partial r'} - \frac{v_\theta'}{r'}\right)^2 + \left(\frac{\partial v_r'}{\partial z'} + \frac{\partial v_z'}{\partial r'}\right)^2 + \left(\frac{\partial v_\theta'}{\partial z'}\right)^2\right]$$

$$- c_{2\varepsilon}\frac{\varepsilon'^2}{k'} \qquad\qquad 3.6$$

The Eqns. 3.1 to 3.6 have been made dimensionless using the dimensionless variables

$$v_r = \frac{v_r'}{U}, \qquad v_z = \frac{v_z'}{U}, \qquad v_\theta = \frac{v_\theta'}{U}$$
as

where, U is the average axial velocity at inlet plane of the nozzle and is defined as

$$U = \frac{Q}{\pi R_1^2}$$

where, Q is the total flow rate through the nozzle.

$$p = \frac{p'}{\rho U^2}, \quad p_1 = \frac{p_1'}{\rho U^2}$$

$$k = \frac{k'}{U^2}, \quad \varepsilon = \frac{2 R_1\, \varepsilon'}{U^3}$$

$$r = \frac{r'}{2R_1}, \quad z = \frac{z'}{2R_1}$$

Finally, the dimensionless forms of Eqns. 3.1 to 3.6 become

**Continuity Equation**

$$\frac{\partial v_r}{\partial r} + \frac{v_r}{r} + \frac{\partial v_z}{\partial z} = 0 \tag{3.7}$$

**Momentum Equations:**

r-Momentum

$$\frac{\partial v_r}{\partial t} + \frac{\partial}{\partial r}\left(v_r^{\,2}\right) + \frac{\partial}{\partial z}\left(v_z\,v_r\right) + \frac{v_r^{\,2} - v_\theta^{\,2}}{r} = -\frac{\partial p_1}{\partial r} + \frac{2}{\mathrm{Re}}\frac{\partial}{\partial r}\left(\mu_{eff}\frac{\partial v_r}{\partial r}\right) +$$
$$\frac{2}{\mathrm{Re}}\frac{\mu_{eff}}{r}\left(\frac{\partial v_r}{\partial r} - \frac{v_r}{r}\right) + \frac{1}{\mathrm{Re}}\frac{\partial}{\partial z}\left\{\mu_{eff}\left(\frac{\partial v_z}{\partial r} + \frac{\partial v_r}{\partial z}\right)\right\} \tag{3.8}$$

z-Momentum

$$\frac{\partial v_z}{\partial t} + \frac{\partial}{\partial r}\left(v_r\,v_z\right) + \frac{\partial}{\partial z}\left(v_z^{\,2}\right) + \frac{v_r\,v_z}{r} = -\frac{\partial p_1}{\partial z} +$$
$$\frac{1}{\mathrm{Re}}\frac{1}{r}\frac{\partial}{\partial r}\left\{r\mu_{eff}\left(\frac{\partial v_z}{\partial r} + \frac{\partial v_r}{\partial z}\right)\right\} + \frac{2}{\mathrm{Re}}\frac{\partial}{\partial z}\left(\mu_{eff}\frac{\partial v_z}{\partial z}\right) \tag{3.9}$$

θ-Momentum

$$\frac{\partial v_\theta}{\partial t} + \frac{\partial}{\partial r}\left(v_r\, v_\theta\right) + \frac{\partial}{\partial z}\left(v_z\, v_\theta\right) + \frac{2v_r\, v_\theta}{r} \quad =$$

$$\frac{1}{\mathrm{Re}}\, \frac{1}{r^2}\, \frac{\partial}{\partial r}\left\{ r^2\, \mu_{eff}\left(\frac{\partial v_\theta}{\partial r} - \frac{v_\theta}{r}\right)\right\} + \frac{1}{\mathrm{Re}}\, \frac{\partial}{\partial z}\left(\mu_{eff}\, \frac{\partial v_\theta}{\partial z}\right) \qquad 3.10$$

where,

$p_1 = p + 2/3\,(k)$

$\mu_{eff} = 1 + \mu_t$

$\mu_t = c_\mu \cdot \mathrm{Re}. \dfrac{k^2}{\varepsilon}$

where, The Reynolds number at inlet to the nozzle $R_e = 2\rho U R_1/\mu$

## Turbulent Kinetic Energy Equation :

$$\frac{\partial k}{\partial t} + \frac{\partial}{\partial r}\left(v_r\, k\right) + \frac{\partial}{\partial z}\left(v_z k\right) + \frac{v_r\, k}{r} = \frac{1}{\mathrm{Re}}\, \frac{1}{r}\, \frac{\partial}{\partial r}\left(r\, \frac{\mu_t}{\sigma_k}\, \frac{\partial k}{\partial r}\right) + \frac{1}{\mathrm{Re}}\, \frac{\partial}{\partial z}\left(\frac{\mu_t}{\sigma_k}\, \frac{\partial k}{\partial z}\right) +$$

$$\frac{1}{\mathrm{Re}}\mu_t \left[ 2\left\{\left(\frac{\partial v_r}{\partial r}\right)^2 + \left(\frac{v_r}{r}\right)^2 + \left(\frac{\partial v_z}{\partial z}\right)^2\right\} + \left(\frac{\partial v_\theta}{\partial r} - \frac{v_\theta}{r}\right)^2 \atop + \left(\frac{\partial v_r}{\partial z} + \frac{\partial v_z}{\partial r}\right)^2 + \left(\frac{\partial v_\theta}{\partial z}\right)^2 \right] - \varepsilon \qquad 3.11$$

## Turbulent Kinetic Energy Dissipation Rate Equation :

$$\frac{\partial \varepsilon}{\partial t} + \frac{\partial}{\partial r}\left(v_r\, \varepsilon\right) + \frac{\partial}{\partial z}\left(v_z\, \varepsilon\right) + \frac{v_r\, \varepsilon}{r} = \frac{1}{\mathrm{Re}}\, \frac{1}{r}\, \frac{\partial}{\partial r}\left(r\, \frac{\mu_t}{\sigma_\varepsilon}\, \frac{\partial \varepsilon}{\partial r}\right) + \frac{1}{\mathrm{Re}}\, \frac{\partial}{\partial z}\left(\frac{\mu_t}{\sigma_\varepsilon}\, \frac{\partial \varepsilon}{\partial z}\right) +$$

$$\frac{1}{\mathrm{Re}}\, c_{1\varepsilon}\, \frac{\varepsilon}{k}\, \mu_t \left[ 2\left\{\left(\frac{\partial v_r}{\partial r}\right)^2 + \left(\frac{v_r}{r}\right)^2 + \left(\frac{\partial v_z}{\partial z}\right)^2\right\} + \left(\frac{\partial v_\theta}{\partial r} - \frac{v_\theta}{r}\right)^2 + \left(\frac{\partial v_r}{\partial z} + \frac{\partial v_z}{\partial r}\right)^2 + \left(\frac{\partial v_\theta}{\partial z}\right)^2 \right]$$

$$- c_{2\varepsilon}\, \frac{\varepsilon^2}{k} \qquad 3.12$$

The empirical constants for Eqns. 3.11 and 3.12 are as follows :

$$c_\mu = 0.09, \quad \sigma_k = 1.0, \quad \sigma_\varepsilon = 1.3, \quad c_{1\varepsilon} = 1.44, \quad c_{2\varepsilon} = 1.92$$

## 3.2 Boundary Conditions

**Inlet :**

$$v_z = \frac{q_r}{\left(\dfrac{R_2}{R1}\right)^2}, \qquad\qquad 0 \langle r \langle R_2 \qquad\qquad\qquad 3.13a$$

$$v_z = \frac{(1 - q_r)}{1 - \left(\dfrac{R_2}{R1}\right)^2}, \qquad\qquad R_2 \langle r \langle R_1 \qquad\qquad 3.13b$$

$$v_\theta = (1 - q_r)\left(\frac{R_1}{R_2}\right)\left(\frac{R_1}{R_T}\right)^2, \qquad\qquad R_2 \langle r \langle R_1 \qquad\qquad 3.13c$$

$$v_r = 0, \, k = k_{in} \, , \, \varepsilon = \varepsilon_{in} \qquad\qquad\qquad\qquad 3.13d$$

The flow ratio ($q_r$) in Eqns. 3.13a to 3.13c is defined as

$$q_r = \frac{\text{flow rate through the central entry port}}{\text{total flow rate through the nozzle}} \qquad\qquad 3.13e$$

**Outlet :**

$$\frac{\partial \varphi}{\partial z} = 0, \quad p = p_a \qquad\qquad\qquad\qquad 3.14$$

where,

$\varphi$ equals to $v_r$ , $v_z$ , $v_\theta$ and k

$p_a$ is ambient pressure

**Wall :**

$$v_r = v_z = v_\theta = 0 \qquad\qquad 3.15$$

Logarithmic Law of wall for turbulent quantities

**Axis of symmetry ( r = 0 ):**

$$\frac{\partial v_z}{\partial r} = v_r = v_\theta = 0 \qquad\qquad 3.16$$

## 3.3 Coefficient of Discharge and Spray Cone Angle

The Coefficient of Discharge and the Spray Cone Angle are determined from

$$C_d = \frac{Q}{A_o \left( \dfrac{2\Delta p'}{\rho} \right)^{\frac{1}{2}}} \qquad\qquad 3.17$$

$$\psi = 2\cos^{-1}\left( \frac{\overline{V}_{zo}}{\left( \overline{V}_{zo}^2 + \overline{V}_{ro}^2 + \overline{V}_{\theta o}^2 \right)^{\frac{1}{2}}} \right) \qquad\qquad 3.18$$

where, the dimensionless average axial, radial and tangential components of liquid velocities at the nozzle exit are determined as

$$\overline{V}_{zo} = \frac{1}{\left( \dfrac{R_o}{R_1} \right)^2} \qquad\qquad 3.19a$$

$$\overline{V}_{ro} = \frac{\displaystyle\int_0^{R_0} r\, V_z\, V_r\, dr}{\displaystyle\int_0^{R_0} r\, V_z\, dr} \qquad\qquad 3.19b$$

$$\overline{V}_{\theta 0} = \frac{\displaystyle\int_0^{R_0} r\, V_z\, V_\theta\, dr}{\displaystyle\int_0^{R_o} r\, V_z\, dr} \qquad\qquad 3.19c$$

26

## 3.4 Numerical Scheme

The velocity and pressure fields were calculated by solving the momentum Eqns. (3.8 to 3.10) along with continuity Eqn. (3.7) satisfying the respective boundary conditions by an explicit finite difference computation technique developed by Hirt and Cook [1972] following the original MAC (Marker and Cell) method due to Harlow and Welch [1965]. The time independent steady state solution of flow was achieved by advancing the equations in time till the temporal derivatives of all the variables were reduced below a pre-assigned small quantity, $\Delta$. The performance parameters were calculated from the velocity and pressure values at the nozzle exit using Eqn. 3.17 and 3.18 once the steady state solution was attained.

The computational domain was divided into a set of small cells. The variables in the domain were defined following a staggered grid arrangement, with the velocity components located at the center of the cell faces and the scalars (p, k, $\varepsilon$ ) located at the cell centers. The cells were labeled with an index (i, j), which denoted the cell number as counted in the positive direction of 'z' and 'r' respectively. A time dependent solution was obtained by advancing the flow field variables through a sequence of a short time step, $\delta t$ calculated in a manner described later. The advancement of the variables was made in two stages. First, all the variables were advanced explicitly based on their values at previous time step and then the velocities calculated in the first stage were corrected to satisfy the mass conservation for each cell an iterative pressure correction $\delta_{i,j}$ introduced in each cell was based on the mass divergence $D_{i,j}$, calculated from the associated velocities with the cell as

$$\delta p_{i,j} = -\frac{\beta D_{i,j}}{\dfrac{\partial D_{i,j}}{\partial p_{i,j}}} \qquad\qquad 3.20$$

where, $\beta$ is an over–relaxation factor.

The idea behind the pressure correction was to conserve the mass by reducing the pressure in the cells having a net positive mass divergence. The change in pressure within a cell changed the associated velocity components as follows

$$(v_r)_{i,j} = (\tilde{v}_r)_{i,j} + \frac{\delta t}{\delta r} \delta p_{i,j}$$
<div align="right">3.21</div>

$$(v_r)_{i,j-1} = (\tilde{v}_r)_{i,j-1} - \frac{\delta t}{\delta r} \delta p_{i,j}$$
<div align="right">3.22</div>

$$(v_z)_{i,j} = (\tilde{v}_z)_{i,j} + \frac{\delta t}{\delta z} \delta p_{i,j}$$
<div align="right">3.23</div>

$$(v_z)_{i-1,j} = (\tilde{v}_z)_{i-1,j} - \frac{\delta t}{\delta z} \delta p_{i,j}$$
<div align="right">3.24</div>

Where, $\bar{\tilde{v}}$ represents the velocity calculated after the first stage calculation as mentioned before.

As the pressure-velocity corrections in one cell affect the pressures and velocities associated with the neighboring cells, the process had to be carried out iteratively, till the mass divergence of all cells was reduced below a small pre-assigned value. The pressure and velocity fields, so corrected, and gave the final solution at the advanced time level. In original MAC method, the pressures in the cells were obtained by solving the Poisson's equation for pressure directly according to Harlow and Welch [1965] . The present method of pressure- velocity coupling was done by iterative method using the principle of conservation of mass , developed by Hirt and Cook [1972] and Hirt et al. [1975] following a related technique developed by Chorin [1967].

## 3.5 Discretization Scheme

The continuity equation (Eqn. 3.7) was discretized following a central differencing scheme. In momentum equations (Eqns. 3.8 to 3.10 ) and k and $\varepsilon$ equations (Eqns. 3.11 and 3.12 ), the space derivatives of the diffusion terms were discretized by central differencing scheme. The advection terms, on the other hand, were discretized by hybrid differencing scheme described by Patankar [1980], where the discretization was made based on the local Peclet number (Pe associated with the cell). A central differencing scheme was adopted when the Peclet number was in the range of $-2 \leq Pe \leq 2$. When the Peclet number was outside the range, an upwind scheme was used in which diffusion terms were set equal to zero.

## 3.6  Grid Specification

A 44X62 variable sized adaptive grid system was considered to make the computational cells finer near the inlet and wall regions. The variations in the size of grids were made uniformly. Grid independence test was done for each set of calculation by doubling and quadrupling the number of grids in both r and z directions and it was found that the changes in the magnitude of the local velocity components and turbulent kinetic energy were not more than 2% .

## 3.7 Time Step Specification

The choice of the time step ($\delta t$) to ensure the stability in the computation was calculated satisfying two restrictions as suggested by Hirt et al. [1975]. First, the fluid should not travel more than one cell in one time step.

$$\delta t_1 \langle \min\left( \frac{\delta z}{|v_z|}, \quad \frac{\delta r}{|v_r|} \right) \qquad\qquad 3.25$$

Therefore, the time step must satisfy the inequality ,

where, the minimum value was calculated with respect to every cell in the mesh. Typically, $\delta t_1$ was chosen to be one-fourth to one-third of the minimum cell transit time obtained from Eqn. 3.25.

Second, the momentum should not diffuse through approximately more than one cell in one time step. A linear stability analysis showed that this limitation implied,

$$\delta t_2 < 0.5 \, Re \, \frac{\delta r^2 \, \delta z^2}{\delta r^2 + \delta z^2}$$
3.26

Finally,
$$\delta t = \min(\delta t_1, \delta t_2)$$
3.27

The required value of $\delta t$, as explained above, was found out at each time level. Often a more stringent restriction on $\delta t$ than given by Eqn. 3.27 was required to have a converged solution and this was fixed by trial and error during the computation.

# CHAPTER 4

## RESULTS AND DISCUSSION

The velocity field within the nozzle has been plotted in r-z (grid 44X62) plane for Re = 1X10 $^4$, $q_r$, = 0.1 and $D_T/D_1$ = 0.21 in Fig.4.1. Fig.4.1 depicts the flow field inside the nozzle of a given geometry and given operating conditions. A recirculation is observed in the annular space at the inlet region of nozzle which does not reach to axis at all. The flow fields at other operating conditions, as studied in the present work, are similar to that as shown in Fig. 4.1.
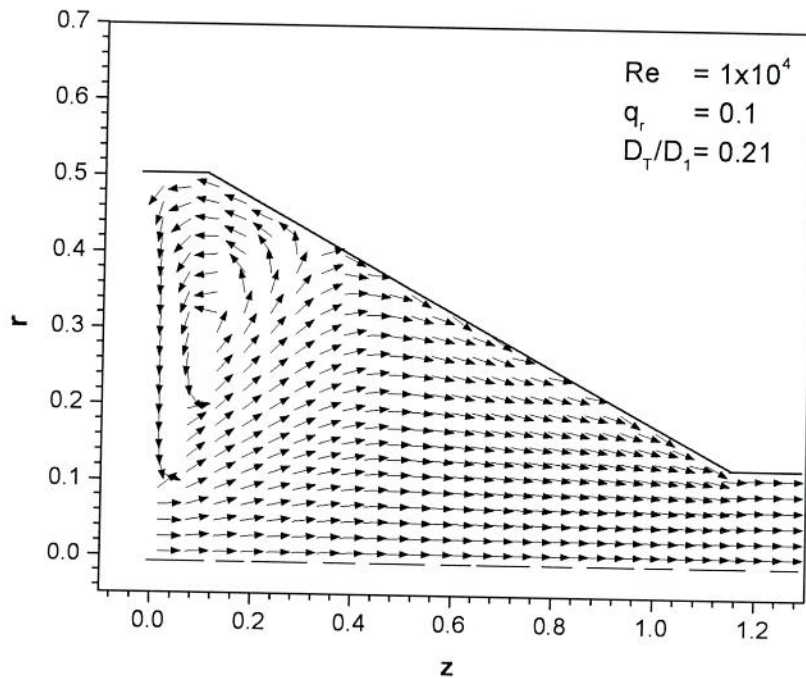
**Fig. 4.1 Velocity field in a solid cone swirl nozzle without a vane swirler**

## 4.1. Influence of Reynolds number Re and $D_T/D_1$ on the coefficient of discharge $C_d$ and the spray cone angle $\psi$.

Coefficient of discharge $C_d$ versus Reynolds number Re and Spray cone angle $\psi$ versus Reynolds number Re are plotted in Fig.4.2 & Fig.4.3 respectively. Reynolds number Re

is varied from $1 \times 10^4$ to $6 \times 10^4$ for $q_r = 0.1$, $D_2/D_1 = 0.17$ and $D_o/D_1 = 0.25$ in both the plots. Two different plots have been made for $D_T/D_1 = 0.21$ and $D_T/D_1 = 0.25$ in both the figures. It has been observed from the numerical computations (Figs 4.2 and 4.3) that the coefficient of discharge $C_d$ remains almost uninfluenced and the spray cone angle $\psi$ decreases with the increase in inlet Reynolds number Re for given values of $D_T/D_1$, $q_r$ and $D_2/D_1$. An increase in Reynolds number Re for a given values of flow ratio $q_r$, $D_2/D_1$ and $D_T/D_1$, implies an increase in the flow through both the central port and the tangential ports proportionately. It causes an increase in both the axial and tangential velocities at inlet to the nozzle. Hence, swirling strength increases at the same time friction in flow also increases and finally results in almost constant values of $C_d$ and a decrease in $\psi$ with Re.

It is further observed (Figs.4.2 and 4.3) that $C_d$ decreases and $\psi$ increases with a decrease in $D_T/D_1$ ratio for fixed values of Re, $q_r$, $D_o/D_1$ and $D_2/D_1$. For given values of Re and $q_r$, a decrease in $D_T/D_1$ causes to increase in the tangential velocity at inlet to the nozzle. Then the pressure drop within the nozzle increases and at the same time the tangential component of velocity also increases over the axial one at the nozzle exit.
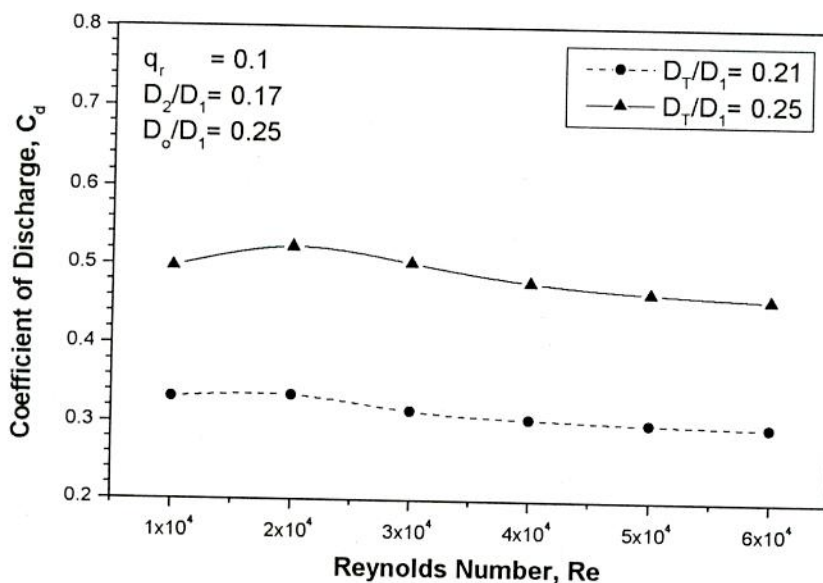


Fig. 4.2 Effects of inlet Reynolds number Re and $D_T/D_1$ on $C_d$
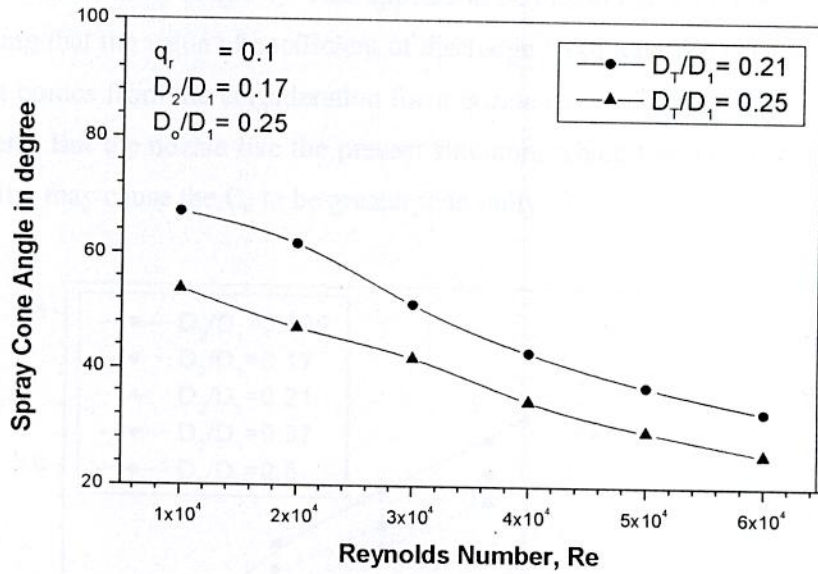
The chart shows Spray Cone Angle in degree (y-axis, 20 to 100) versus Reynolds Number, Re (x-axis, $1\times10^4$ to $6\times10^4$).

Conditions shown on chart:
$q_r = 0.1$
$D_2/D_1 = 0.17$
$D_o/D_1 = 0.25$

Legend:
$D_T/D_1 = 0.21$
$D_T/D_1 = 0.25$

**Fig. 4.3 Effects of inlet Reynolds number Re and $D_T/D_1$ on $\psi$**

## 4.2. Influence of flow ratio $q_r$ and diameter ratio $D_2/D_1$ on the coefficient of discharge $C_d$ and the spray cone angle $\psi$.

Coefficient of discharge $C_d$ versus flow ratio $q_r$ is plotted in Fig.4.4. Flow ratio $q_r$ is varied from 0.1 to 0.5 for Re = $5\times10^4$, $D_T/D_1 = 0.21$ and $D_o/D_1 = 0.25$. Five different plots have been plotted for $D_2/D_1 = 0.125$, 0.17, 0.21, 0.37 and 0.5. It is observed from the numerical predictions (Fig. 4.4) that the coefficient of discharge $C_d$ increases slightly with the flow ratio $q_r$ for a given value of Re, $D_o/D_1$ and $D_T/D_1$, at higher values of diameter ratios ( $D_2/D_1 = 0.37$ to 0.5 ). But when $D_2/D_1$ is decreased below 0.37 the value of $C_d$ increases sharply with an increase in $q_r$. An increase in the value of flow ratio $q_r$ for a given value of Re, implies an increase in flow through the central port and a reduction in flow through the tangential ports at inlet to the nozzle. This causes an increase in the average axial velocity through the central port and a decrease in tangential velocity at the inlet. Under this situation, the swirling strength of flow within the nozzle is reduced with a subsequent reduction in the pressure drop for a given flow. This results in an increase in the value of $C_d$ and a decrease in $\psi$.

port at nozzle inlet is considerably reduced while the tangential velocity is increased. This causes an increased strength of swirl in the flow through the nozzle and finally results in a higher value of $\psi$.
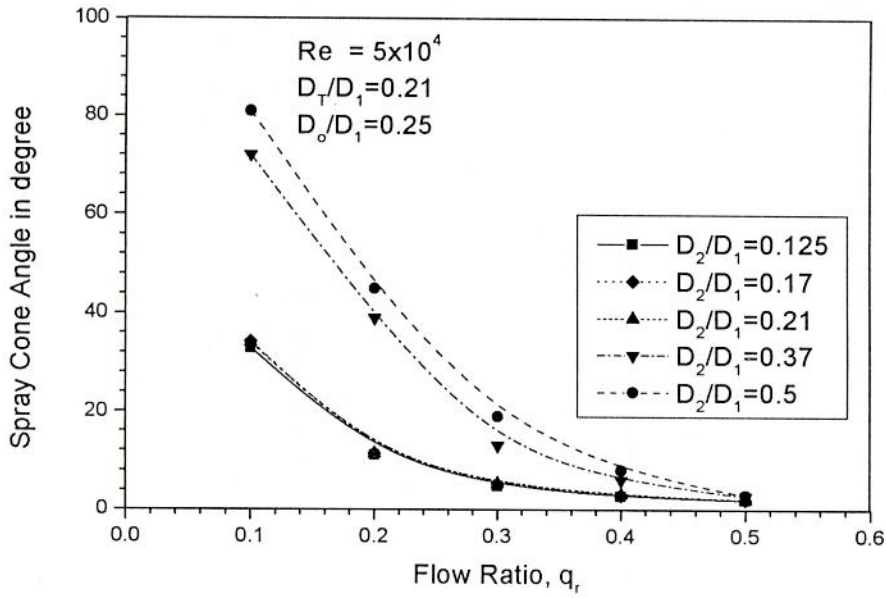


**Fig. 4.5 Effects of flow ratio $q_r$ and diameter ratio $D_2/D_1$ on $\psi$**

## 4.3. Comparison of numerical predictions from present work with the published results

The comparisons of numerically predicted values from the present work with the published results of other authors are as follows-

The coefficient of discharge $C_d$ from the present work is found less while the $\psi$ is found higher than that of published results of Halder et al. [2004]. The maximum variation of coefficient of discharge $C_d$ and spray cone angle $\psi$ values from the present work for the effect of flow Reynolds number Re for a given values of $D_o/D_1$, $q_r$ and $D_2/D_1$ were 10.5% and 43.1% respectively. While the same from Halder et al.'s [2004] results were 6.45% and 10.9% respectively for the same working range.

$D_2/D_1$ were 10.5% and 43.1% respectively. While the same from Halder et al.'s [2004] results were 6.45% and 10.9% respectively for the same working range.

The maximum variation of coefficient of discharge $C_d$ and spray cone angle $\psi$ values from the present work for the effect of flow ratio $q_r$ for a given values of $D_T/D_1$, Re and $D_2/D_1$ (0.125 to 0.21) were 66.47% and 87.87% respectively. While the same from Halder et al. [2004]'s results were 46.5% and 75% respectively for the same working range.

Although the comparison has been made between two works but both works have not been done in the same environment. In Halder et al. [2004]'s work, swirling strength was generated by applying swirl number while the same is generated in the present work by applying tangential flow through tangential entry ports. But the trends of variation of coefficient of discharge $C_d$ and spray cone angle $\psi$ in both the cases are found similar. Moreover, higher values of spray cone angle $\psi$ as obtained in the present work could be able to provide better atomization than the nozzle with a vane swirler.

# CONCLUSIONS

Modeling of flow through a solid cone nozzle without a vane swirler has been made in the present project. The performance parameters like coefficient of discharge $C_d$ and spray cone angle $\psi$ have been predicted from numerical solution as functions of nozzle geometry and injection conditions. The coefficient of discharge $C_d$ is almost uninfluenced and the spray cone angle $\psi$ decreases with the increase of Reynolds number Re of flow at inlet to the nozzle for a given values of $q_r$, $D_o/D_1$ and $D_2/D_1$. A decrease in $D_T/D_1$ ratio for a given Re, $q_r$ $D_o/D_1$ and $D_2/D_1$ decreases the coefficient of discharge $C_d$ and increases the spray cone angle $\psi$. An increase in the value of flow ratio $q_r$ for a given Re, $D_T/D_1$ and $D_2/D_1$ increases the coefficient of discharge $C_d$ but decreases the spay cone angle $\psi$. The solid cone nozzles with or without a vane swirler show similar trends of variation of performance parameters like $C_d$ and $\psi$. In some cases, the nozzle without a vane swirler produces higher spray cone angle than that of nozzle with a vane swirler. The nozzle assumed for the present work would be less costly and provides higher spray cone angle $\psi$ which could produce better atomization as well.

# REFERENCES

Binnie, A.M. and Harris, D.P., 1950. **The Application of Boundary Layer Theory to Swirling Flow Through a Nozzle.** Quart. J. Mech. and Appl. Math. , **Vol. 3**, p. 89.

Binnie, A.M., 1951. **The Theory of Waves Travelling on the Core in a Swirling Liquid.** Proc. Roy. Soc. (London), **Vol. 205**, p. 530.

Binnie, A.M. and Teare, J.D., 1956**. Experiments in the Flow of a Swirling Water Through a Pressure Nozzle and an Open Trumpet.** Proc. Roy. Soc. (London), **A 235**.

Binnie, A.M., Hakings, G.A. and Kamel, M.Y.M., 1957**. The Flow of Swirling Water Through a Convergent-Divergent Nozzle.** J. Fluid Mech., **Vol. 3**, p. 261.

Chang, K.C. and Chen, C.S., 1993. **Development of a Hybrid k-ε Turbulence Model for Swirling Recirculating Flows under Moderate to Strong Swirl Intensity.** Int. J. Numerical Methods in Fluids, **Vol. 16**, p. 421.

Chen, S.K., Lefebvre, A.H. and Rollbuhler, J., 1992. **Factors Influencing the Effective Spray Cone Angle of Pressure Swirl Atomisers.** ASME J. Engg. for Gas Turbine and Power**, Vol. 114**, p. 97.

Chorin, A.J., 1967. **A Numerical Method for Solving Incompressible Viscous Flow Problem.** J. Comp. Phys., **Vol. 2**, p. 12.

Cooke, J.C., 1952. **On Pohlhausen's Method with Application to a Swirl Problem of Taylor.** J. Aero. Sci., **Vol. 19**, p. 486.

Datta, A. and Som, S.K., 2000. **Numerical Prediction of Air Core Diameter, Coefficient of Discharge and Spray Cone Angle of a Swirl Spray Pressure Nozzle.** Int. J. Heat and Fluid Flow, **Vol. 21**, P. 412.

Fu, S., Huang, P.G., Launder, B.E. and Leschziner, M.A., 1988. **A Comparison of Algebraic and Differential Second- Moment Closures for Axisymmetric Turbulent Shear Flows with and without Swirl.** ASME J. Fluids Engg., **Vol. 110,** p. 216.

Giffen, E. and Massey, B.S., 1950. **Some Observations on Flow in Spray Nozzles.** Motor Industry Res. Assoc., Report No. 1948/4.

Halder, M.R., Dash, S.K. and Som, S.K. 2002. **Initiation of Air Core in a Simplex Nozzle and the Effects of Operating Geometrical Parameters on its Shape and Size.** Int. J. Expt. Thermal and Fluid Sc., **Vol. 26,** p. 871.

Halder, M.R., Dash, S.K. and Som, S.K. 2003. **Influence of Nozzle Flow and Nozzle Geometry on the Shape and Size of a Air Core in a Hollow Cone Swirl Nozzle.** Proc. Instn Mech. Engrs Vol **217** Part C: Int. J. Mechanical Engineering Science, p. 207.

Halder, M.R., Dash, S.K. and Som, S.K., 2004. **A Numerical and Experimental Investigation on the Coefficient of Discharge and the Spray Cone Angle of a Solid Cone Swirl Nozzle.** Int. J. Experimental Thermal and Fluid Science, **Vol. 28**, p. 297.

Harlow, F.H. and Welch, J.E., 1965. **Numerical Computation of Time Dependent Viscous Incompressible Flow of Fluid with a Free Surface.** Phys. Fluid , **Vol. 8 (12)**, p.2182.

Hirt, C.W. and Cook, J.L., 1972. **Calculating Three-Dimensional Flows Around Structure and Over Round Terrain.** J.Comp. Phys., **Vol. 10**, p.324.

Hirt, C.W., Nicholas, B.D. and Romero, N.C., 1975. **SOLA- A Numerical Solution Algorithm for Transient Fluids Flows.** Los. Almos Scientific Lab., Rep. LA 5852.

Holtzclaw, D., Sakman, T., Jeng, S.M., Jog, M.A. and Benjamin, M.A., 1997. **Investigation of Flow in a Simplex Fuel Nozzle.** AIAA Paper 97, p. 2970.

Jones, A.R., 1982. **Design Optimisation of a Large Pressure Jet Atomiser for Power Plant.** In: Proceedings of the Second International Conference on Liquid Atomisation and Spray Systems, p. 181.

Jones, W.P and Pascau, A., 1989**. Calculation of confined Swirling Flows with a Second Moment Closure.** ASME J. Fluids Engg., **Vol. 111**, p. 248.

Kutty, S.P., Narasimhan, M. and Narayanaswamy, K., 1978**. Design and Prediction of Discharge Rate, Cone Angle and Air Core Diameter of Swirl Chamber Atomisers.** In: Proceedings of the first International Conference on Liquid Atomisation and Spray systems, p. 93.

Launder, B.E., Piriddin, C.H. and Sharma, B.I., 1977. **The Calculation of Turbulent Boundary Layers on Spinning and curved Surfaces.** ASME J. Fluids Engg., **Vol. 99**, p. 412.

Lefebvre, A.H., 1989. **Atomization and Sprays.** Hemisphere Publishing Corporation, Washington, DC.

Liao, Y., Sakman, A.T., Jeng, S.M., Jog, M.A. and Benjamin, M.A., 1999. **A Comprehensive Model to Predict Simplex Atomizer Performance.** ASME J. Engg. for Gas Turbine and Power, **Vol. 121**, p. 285.

Nasr, G.G., Sharief, R., James, D.D., Jeong, J.R, Widger, I.R. and Yule, A.J. **Studies of high pressure water sprays from full cone atomizers.** Proc. ILLAS-Europe'99, Toulouse 5-7 July, 1999.

Nikjooy, M. and Mongia, H.C., 1991**. A Second- Order Modelling Study of Confined Swirling Flows.** Int. J. Heat and Fluid Flow, **Vol. 12**, p. 12.

Nissan, A.H. and Breason, V.P., 1961. **Swirling flow in Cylinreds**. A.I.Ch.E Journal, **Vol. 7**, p. 543.

Patankar, S.V., 1980. **Numerical Heat Transfer and Fluid Flow,** Hemisphere Publishing Corporation, washington, D.C.

Radcliffe, A., 1955. **The Performance of a Type of Swirl Atomizer.** Proceedings, Inst. of Mech. Engrs. (London), **Vol. 169**, p. 93.

Rizk, N.K. and Lefebvre, A.H., 1985a. **Internal Flow Characteristics of Simplex Swirl Atomizers.** AIAA J. Propul. and Power, **Vol. 1 (3)**, p. 193.

Rizk, N.K. and Lefebvre, A.H., 1985b. **Prediction of Velocity Coefficient and Spray Cone Angle for Simplex Swirl Atomizers.** In: Proceedings of the Third International Conference on Liquid Atomization and Spray systems, p. 111c/2/1.

Rodi, W., 1979. **Influence of Buoyancy and Rotation of Equations for the Turbulent Length Scale.** Proc. 2$^{nd}$ Symp. on Turbulent Shear Flows, Imperial College, London, p. 10.37.

Sakman, A.T., Jog, M.A., Jeng, S.M. and Benjamin, M.A., 2000. **Parametric Study of Simplex Fuel Nozzle Internal Flow and Performance.** AIAA J., **Vol. 38 (7)**, p. 1214.

Som, S.K. 1983a., **Theoretical and Experimental Investigations on the Formation of Air Core in a Swirl Spray Atomising Nozzle Using Power Law Non-Newtonian Liquid.** Appl. Scientific Res., **Vol. 40**, p. 71.

Som, S.K. 1983b., **Theoretical and Experimental Investigations on the Coefficient of Discharge and Spray Cone Angle of a Swirl Atomising Nozzle Using Power Law Non-Newtonian Fluid.** J. non-Newtonian E. Mech., **Vol. 12**, p. 39.

Som, S.K. and Mukherjee, S.G., 1980. **Theoretical and Experimental Investigations on the Formation of Air Core in a Swirl Spray Atomising Nozzle.** Appl. Scientific Res, **Vol. 36**, p. 173.

Som, S.K. and Mukherjee, S.G., 1980b. **Theoretical and Experimental Investigations on the Coefficient of Discharge and Spray Cone Angle of a Swirl Atomizing Nozzle.** Acta. Mechanica, **Vol. 36**, p. 79.

Steinthorsson, E., and Lee, D.M., 2000. **Numerical Simulation of Internal Flow in a Simplex Atomizer.** In Eighth International Conference on Liquid Atomization and Spray Systems, Pasadena, CA, USA.

Suyari, M and Lefebvre, A.H., 1986. **Flim Thickness Measurements in a Simplex Swirl Atomizer.** AIAA J. Propul. and Power, **Vol. 2**, No. **6**, p.528.

Sturgess, G.J. and Syed, S.A., 1990. **Calculation of Confined Swirling Flows.** Int. J. Turbo Jet Engines, **Vol. 7**, p. 103.

Talbot, L., 1954. **Laminar Swirling Pipe Flow.** J .Appl.Mech., **Vol. 21**, p.1.

Tate, R.W. and Marshall, W.R., 1953. **Atomization by Centrifugal Nozzles**. J. Chem. Engg. Prog., 49, p. 169.

Taylor, G.I., 1948**. The mechanics of a swirl atomizers**. In: Proceedings of the Seventh International Congress for Applied Mechanics, **Vol. 2 (1)**, p. 280.

Taylor, G.I., 1950. **The Boundary Layer in the Converging Nozzle of Swirl Atomizer.** Quart. J. Mech. Appl. and Math., **Vol. 3**, p.129.

Walmsley, S.J., Watkins, A.P. and Yule, A.J. **On the prediction and structures of wide angle full cone liquid sprays.** Proc. ILLAS-Europe,2000, Darmstadt 11-13 Sept.,2000.

$D_2/D_1$ were 10.5% and 43.1% respectively. While the same from Halder et al.'s [2004] results were 6.45% and 10.9% respectively for the same working range.

The maximum variation of coefficient of discharge $C_d$ and spray cone angle $\psi$ values from the present work for the effect of flow ratio $q_r$ for a given values of $D_T/D_1$, Re and $D_2/D_1$ (0.125 to 0.21) were 66.47% and 87.87% respectively. While the same from Halder et al. [2004]'s results were 46.5% and 75% respectively for the same working range.

Although the comparison has been made between two works but both works have not been done in the same environment. In Halder et al. [2004]'s work, swirling strength was generated by applying swirl number while the same is generated in the present work by applying tangential flow through tangential entry ports. But the trends of variation of coefficient of discharge $C_d$ and spray cone angle $\psi$ in both the cases are found similar. Moreover, higher values of spray cone angle $\psi$ as obtained in the present work could be able to provide better atomization than the nozzle with a vane swirler.